IJRCS

International Journal of Robotics and Control Systems
Vol. 1, No. 4, 2021, pp. 416-427
ISSN 2775-2658
http://pubs2.ascee.org/index.php/ijrcs

ASCEE

Maximum Torque per Ampere Control of Permanent Magnet Assisted Synchronous Reluctance Motor: An Experimental Study

Yasmine Ihcene Nadjai [a,1], Hafiz Ahmed [b,2], Noureddine Takorabet [c,3], Peyman Haghgooei [c,4]

[a] Department of Electrical Engineering, National Polytechnic School, 16200 Algiers, Algeria
[b] Nuclear Futures Institute, Bangor University, Bangor LL57 2DG, United Kingdom
[c] GREEN - Université de Lorraine 54500 Vandœuvre-lès-Nancy, France
[1] nadjaiyasmine@gmail.com, [2] hafiz.ahmed@bangor.ac.uk, [3] noureddine.takorabet@univlorraine.fr,
[4] peyman.haghgooei@univlorraine.fr
* Corresponding Author

ARTICLE INFO

Article history
Received 15 September 2021
Revised 24 September 2021
Accepted 23 October 2021

Keywords
Copper Loss;
Permanent Magnet Assisted Reluctance Motor;
Motor Control;
Maximum Torque per Ampere

ABSTRACT

In recent times, permanent magnet assisted synchronous reluctance motors (PMaSRM) have been considered as suitable traction motors for electric vehicle applications. In this type of machine, where the share of reluctance torque is more significant than the excitation torque, it is more appropriate to use a control strategy that can fully utilize the reluctance torque. This paper deals with a new structure of permanent magnet-assisted synchronous reluctance motors that was designed and manufactured in a previous study. This paper suggests applying, in a first study, a constant parameter maximum torque per ampere (MTPA) strategy to make a contribution towards the control of such structure that is becoming increasingly attractive in the field of electric transportation. This method is usually used to control interior permanent magnet synchronous motors to minimize the copper losses of the system. Before implementing and simulating this method, the mathematical models of the suggested motor and the inverter are given. An experimental study is conducted on a small-scale 1 kW prototype PMaSRM using a MicrolabBox Dspace to test and examine the proposed control. Simulation and experimental results are presented in this article in order to verify the validity of the developed control strategy.

1. Introduction

Electrified transportation, especially electric vehicles, are going to play a big role towards achieving the net-zero emission by 2050. Currently, most electric vehicles use permanent magnet synchronous motors since they can provide high power and torque density together with good efficiency. However, the rare earth magnets used in those motors are becoming increasingly expressive over the last few years. Moreover, this is also not sustainable. To overcome this issue, machine designers are taking many approaches to develop motors with a reduced amount of permanent magnets without compromising their required performances.

Among the various alternative solutions available in the literature, permanent magnet assisted synchronous reluctance motors (PMaSRM) appear to be a very suitable choice for electric vehicle propulsion applications. The electromagnetic torque of this machine has two components; one is called permanent magnet torque generated by the interaction between the rotor magnetic field and the stator's windings magnetomotive force (or current), while the other is the reluctance torque. Because the d- and q-axis stator current contribute to torque generation, there are different possible combinations of these currents for the desired torque [1][2].

To improve the system's efficiency and reduce motor losses, various control strategies can be adopted, such as unit power factor control [3], $i_c = 0$ control, and maximum torque per Ampere Control (MTPA) [4]. The maximum torque per-ampere is a control technique that has been subject to much research as it focuses on producing the required torque using the minimum current magnitude, which helps to reduce copper losses [5]. The review of the literature reveals that in the majority of existing studies, MTPA strategy is applied to control permanent interior magnet synchronous machine (IPMSM) in order to exploit the double torque generation in the most effective way. The work in [6][7] presents results of the MTPA control when using nominal values for motor parameters. However, parameter variations can be a considerable challenge when implementing the technique. That's why online motor parameter estimation has been suggested in reference [8]–[10] to overcome this issue.

Unlike the IPMSM, the permanent magnet assisted synchronous motor is a motor where the share of reluctance torque is more significant compared to the PM electric torque. To make a contribution towards the control of a structure of motor that is becoming increasingly attractive, this paper suggests the use of the MTPA control technique. The structure and the design of the motor are proposed in [11]. In this first article, only the constant parameter MTPA technique is considered. Mathematical modeling, control design, and experimental results are presented to verify the validity of the developed method.

The rest of this paper is organized as follows: Section II describes the considered motor and also presents the mathematical model of the motor. Details of the developed MTPA control strategy are given in Section III. Simulation results are given in Section IV, while experimental results are provided in Section V. Finally, Section VI concludes this paper

2. Permanent Magnet assisted Synchronous Reluctance Motor Model

2.1. PMaSRM Mathematic Model

The PMaSRM motor has three stator windings and a permanent magnet on the rotor that can be illustrated in the *abc* frame as shown in Fig. 1.

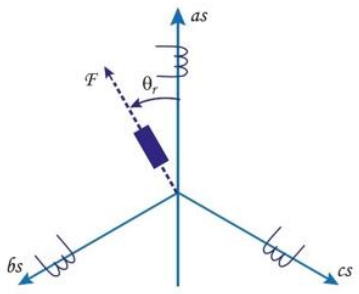

Fig. 1. The three-phase model of the permanent magnet assisted synchronous reluctance motor: three stator windings and a permanent magnet on the rotor

The mathematic model of this motor in the natural frame of reference (ABC frame) in matrix notation is given by the following equations [12]:

- The voltage equation:

$$[V_{abc}] = [R_s].[i_{abc}] + \frac{d[\Psi_{abc}]}{dt} \quad (1)$$

- The flux linkage equation:

$$[\Psi_{abc}] = [L_s].[i_{abc}] + [\Psi_m] \quad (2)$$

Where V_{abc}, i_{abc}, Ψ_{abc} are the phase voltage vector, the stator current vector and the flux linkage vector, $[R_s]$ is the stator resistance matrix, $[Ls]$ is the inductance matrix and $[\Psi_m]$ is the magnitude of the flux linkage established by the permanent magnet. They are defined as follows:

$$[R_s] = \begin{bmatrix} R_s & 0 & 0 \\ 0 & R_s & 0 \\ 0 & 0 & R_s \end{bmatrix}, \quad [\Psi_m] = \begin{bmatrix} \Psi_{ma} \\ \Psi_{mb} \\ \Psi_{mc} \end{bmatrix} = \Psi'_m \begin{bmatrix} cos(\theta) \\ cos\left(\theta - \frac{2\pi}{3}\right) \\ cos\left(\theta - \frac{4\pi}{3}\right) \end{bmatrix}, \quad [L_s] = \begin{bmatrix} L_a & M_{ab} & M_{ac} \\ M_{ba} & L_b & M_{bc} \\ M_{ca} & M_{cb} & L_c \end{bmatrix}$$

Using Clark transformation followed by Park transformation, it is possible to get the mathematic model in the dq frame [13]. Fig. 2 illustrates the definition of d-axis and q-axis of the permanent magnet assisted synchronous reluctance motors used in this work

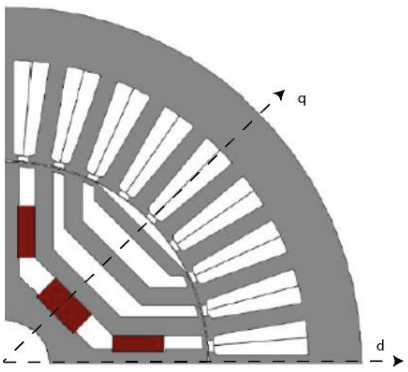

Fig. 2. The d and q axis of the permanent magnet assisted synchronous reluctance motors

In this PMaSRM topology, the magnets are placed along the q-axis rather than d-axis. In the dq reference frame, the stator voltage equations are expressed as follows:

$$V_d = R_s i_d + \frac{d\Psi_d}{dt} - p\omega_r \Psi_q \quad (3)$$

$$V_q = R_s i_q + \frac{d\Psi_q}{dt} + p\omega_r \Psi_d \quad (4)$$

Where Ψ_d and Ψ_q are respectively the flux linkage along d axis and q axis, p is the number of pole-pairs, ω_r is the mechanical angular speed and R_s is the stator resistance. Since the magnets are inserted along the q axis, the equations of flux linkage in dq axis are given by:

$$\Psi_d = L_d i_d \quad (5)$$

$$\Psi_q = L_q i_q - \Psi_m \quad (6)$$

Where L_d is the d-axis inductance, L_q the q-axis inductance and Ψ_m the flux linkage of permanent magnets. By substituting the flux linkage equations (5) and (6) in (3) and (4), the dq-axis motor current dynamics can be obtained as:

$$\frac{di_d}{dt} = \frac{1}{L_d}(V_d - R_s i_d + p\omega_r L_q i_q - p\omega_r \Psi_m) \quad (7)$$

$$\frac{di_q}{dt} = \frac{1}{L_q}(V_q - R_s i_q - p\omega_r L_d i_d) \quad (8)$$

Assuming that the motor parameters are constant (Table 1), the generated electromagnetic torque can be expressed in the dq reference frame by:

$$T_{em} = p(\Psi_d i_q - \Psi_q i_d) \quad (9)$$

Substituting (5) and (6) in (9), the torque equation can be found as:

$$T_{em} = p\{\Psi_m i_d + (L_d - L_q) i_q i_d\} \quad (10)$$

In order to control the motor, it is important to consider its dynamic behavior. The relation between electrical torque and load torque is given by the mechanical equation, which is:

$$J\frac{d\Omega}{dt} = T_{em} - T_r - f\Omega \quad (11)$$

Where J is the inertia of the motor and coupled load, T_r is the load torque and f is the friction coefficient, and Ω is the mechanical angular speed.

Table 1. PMA-SynRM Parameters Based on FEM Analysis

Symbol	Meaning	Value
Ψ_m	Permanent magnet flux	0.138 Wb
L_d	d-axis inductance	288mH
L_q	q-axis inductance	38mH

2.2. Inverter Mathematic Model

The three-phase inverter used to drive the PMaSRM is fed by a DC voltage source and has three-phase legs, each comprised of two switches, as shown in Fig. 3.

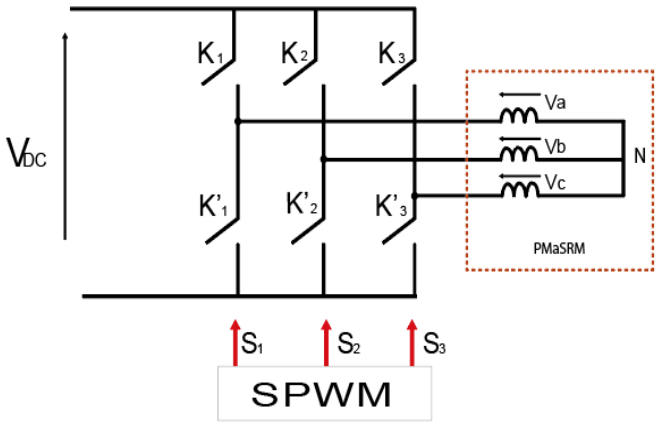

Fig. 3. Three phases inverter driving the PMaSRM, where V_{DC} is the Dc bus voltage, and V_a V_b V_c are phase voltages

The switches are controlled by using sinusoidal pulse width modulation (SPWM) [6] control by comparing a sinusoidal wave and a triangular carrier signal that has a frequency of 10kHz. For each leg of the inverter, we define three connection function S_i $(i = 1, 2, 3)$ [14][15]:

$$S_i = \begin{cases} 1 & \text{if } K_i \text{ is on and } K_i' \text{ is off} \\ 0 & \text{if } K_i \text{ is off and } K_i' \text{ is on} \end{cases} \quad (12)$$

Where K_i and K_i' are switches. The line voltages of the inverter can be expressed by:

$$\begin{cases} U_{ab} = V_{Dc}(S_1 - S_2) \\ U_{bc} = V_{Dc}(S_2 - S_3) \\ U_{ca} = V_{Dc}(S_3 - S_1) \end{cases} \quad (13)$$

The relationship between line voltages and phase voltages are given by:

$$\begin{cases} V_a = \dfrac{U_{ab} - U_{ca}}{3} \\ V_b = \dfrac{U_{bc} - U_{ab}}{3} \\ V_c = \dfrac{U_{ca} - U_{bc}}{3} \end{cases} \quad (14)$$

From (13) and (14), the output phase voltages can be expressed using the connection functions c as following [16]

$$\begin{cases} V_a = \dfrac{V_{Dc}}{3}(2S_1 - S_2 - S_3) \\ V_b = \dfrac{V_{Dc}}{3}(2S_2 - S_1 - S_3) \\ V_c = \dfrac{V_{Dc}}{3}(2S_3 - S_1 - S_2) \end{cases} \quad (15)$$

3. MTPA Control Strategy

The objective of the MTPA control strategy (maximum torque per ampere) is to find, for a given torque, the minimum value of currents, i_d and i_q. To fully understand this principle, the electromagnetic torque versus current angle, according to the different current amplitude, are illustrated in Fig. 4. For each current Amplitude, it can be seen that there is a specific value of the current angle for which the torque reaches its maximum value [17]–[19].

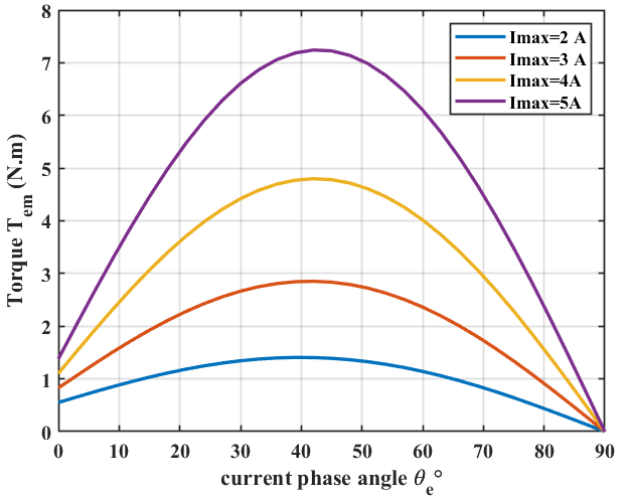

Fig. 4. Relationship between the average torque and the current angle

3.1. Constant Parameter MTPA Control

For a given torque, there are numerous possible combinations of i_d and i_q. Among the possible solutions, there's one pair that can minimize the current magnitude. Ignoring the variation of the motor parameters, finding the optimal solution requires solving the following optimization problem:

$$\begin{cases} min\, I_s = \sqrt{i_d^2 + i_q^2} \\ s.t.\ T_{em} = p\left(\Psi_m i_d + \left(L_d - L_q\right) i_q i_d\right) = const. \end{cases} \tag{16}$$

It can also be stated as:

$$\begin{cases} min\, I_s = \sqrt{i_d^2 + i_q^2} \\ s.t.\ T_{em} = p\left(\Psi_m i_d + \left(L_d - L_q\right) i_q i_d\right) = const. \end{cases} \tag{17}$$

To obtain the current expressions for the maximum torque, the differentiation of torque is made equal to zero as shown in equation (17) [18][20] as

$$\begin{cases} \dfrac{\partial(\mathrm{T_{em}}/I_s)}{\partial \mathrm{i_d}} = 0 \\ \dfrac{\partial(\mathrm{T_{em}}/I_s)}{\partial \mathrm{i_q}} = 0 \end{cases} \tag{18}$$

Keeping the stator current constant and substituting (10) and $I_s = \sqrt{i_d^2 + i_q^2}$ into equation (17), the relationship between i_d and i_q can be written as:

$$i_{q_{opt}} = \frac{-\Psi_m + \sqrt{(\Psi_m)^2 + 4\left(L_d - L_q\right)^2 i_d^2}}{2(L_d - L_q)} \tag{19}$$

For any given torque, it is possible to find the optimal i_d and i_q that reduce the copper losses. As mentioned previously, the motor parameters (L_d, L_q, Ψ_m) are considered constant, and the effect of saturation, as well as temperature influence, are neglected in all the analytical approaches.

3.2. Implementation of MTPA

The block diagram of the PMaSRM drive with MTPA control is illustrated in Fig. 5. To implement the MTPA control method, d-axis and q-axis stator currents need to be controlled according to their references i_d^*, i_q^*. In this study, the reference for the d axis is calculated using the following torque equation:

$$i_d^* = \frac{T_{em}^*}{p\left(\Psi_m + \left(L_d - L_q\right) i_q\right)} \tag{20}$$

Where i_q is the measured q-axis stator current and T_{em}^* is the reference torque generated by the PI controller after comparing the actual speed with the given speed. For the q-axis current, the reference is given by the equation (16) [21][22].

It is to be noted here that It is possible to find from the d-axis and q-axis current reference the relationship between torque and current through Matlab two-dimensional curve fitting function [5][19].

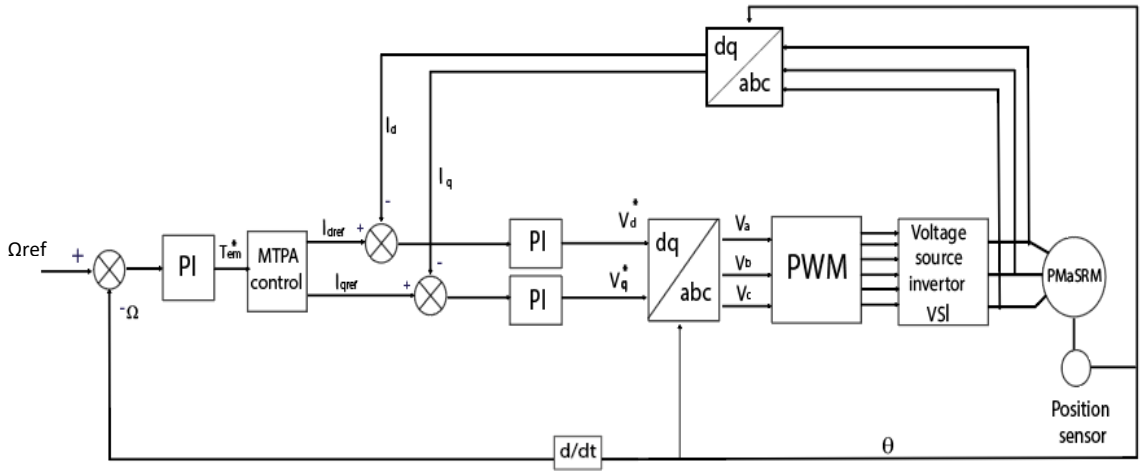

Fig. 5. The block diagram of the PMaSRM drive with MTPA control

The most common approach in the implementation of d-q axis current and speed control loops is the use of proportional-integral controllers. The conventional PI control process is written in the form of the transfer function as:

$$G(s) = k_p + k_i \frac{1}{s} \tag{21}$$

Where k_p is the proportional action coefficient and k_i is the integral action coefficient. By simply adjusting those two parameters, the drive can quickly respond to errors between the command and the actual value. In this study, the PI controllers have been designed following reference [23], where it is possible to determine the gains in a simple way using motor parameters. All parameters used for the simulation are presented in Table 2.

Table 2. PMaSRM/inverter specification and speed/current regulation parameters

Symbol	Meaning	Value
i_{rated}	Rated current	5.4 A
P_{rated}	Rated power	1kW
p	Number of pole pairs	2
R_s	Resistance	3.2 Ω
J	Equivalent inertia	0.0017 kg m^2
f	Friction coefficient	0.0027 Nm s/rad
K_{pd}	d-axis current proportional gain	19.2
K_{pd}	d-axis current integral gain	1.2×10^3
K_{pq}	q-axis current proportional gain	19.2
K_{iq}	q-axis current integral gain	1.5×10^3
$K_{p\Omega}$	Speed-proportional gain	0.2
$K_{i\Omega}$	Speed integral gain	2
V_{Dc}	DC bus voltage	400 V
f_s	Switching frequency	16 Hz

4. Results and Discussion

4.1. Simulation results

In this Section, Matlab/Simulink-based simulation study is reported. Parameters of the PMaSRM are given in Table 1. This paper simulates MTPA control of PMaSRM in two parts, a no-load acceleration phase and a constant speed phase where a load torque is added.

After applying a reference speed of 500 rpm, the motor speed follows this given value with a slight reduction due to load variation, which is quickly adjusted. Under no-load operation, the motor produces an electromagnetic torque that overcomes the friction, and both d-axis and q-axis currents are used for overcoming the inertia. Speed, torque, and current waveforms under no-load operation can be seen in Fig. 6 between 0 and 1s.

When a load is introduced (Tr=2.5 Nm), the current and torque values change, as shown in Fig. 6. The system uses both d-axis and q-axis currents to produce the reference torque with the most effective way to have the lowest stator current resulting in reduced copper losses.

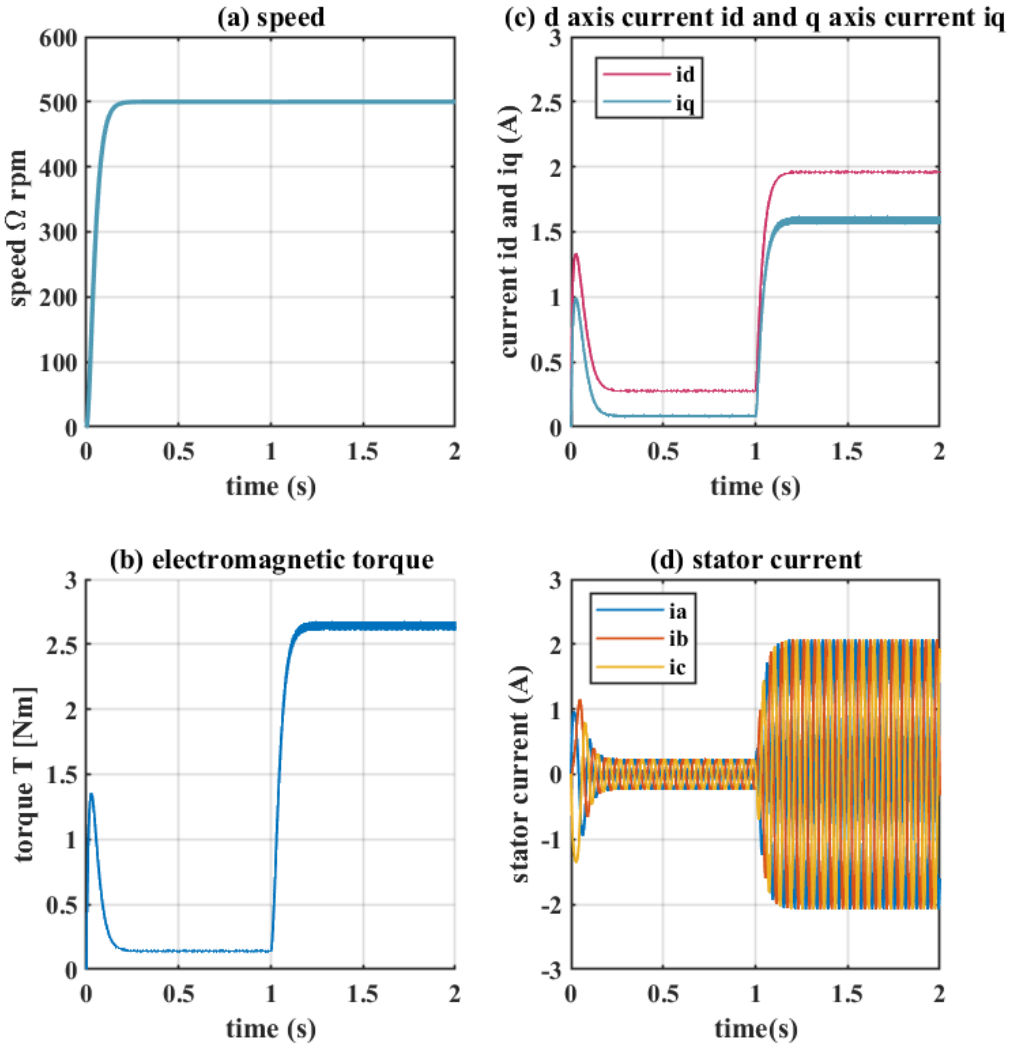

Fig. 6. Simulation results of MTPA Control (a) speed, (b) electromagnetic torque (c) d q current and (d) stator current

It is important to note that for a salient motor, it is more appropriate to use the MTPA control strategy as it can fully utilize the reluctance torque.

4.2. Experimental Results

The experimental study was carried out in in France, in Groupe de Recherche en Energie Electrique (GREEN) laboratory. The test bench is given in Fig. 7.

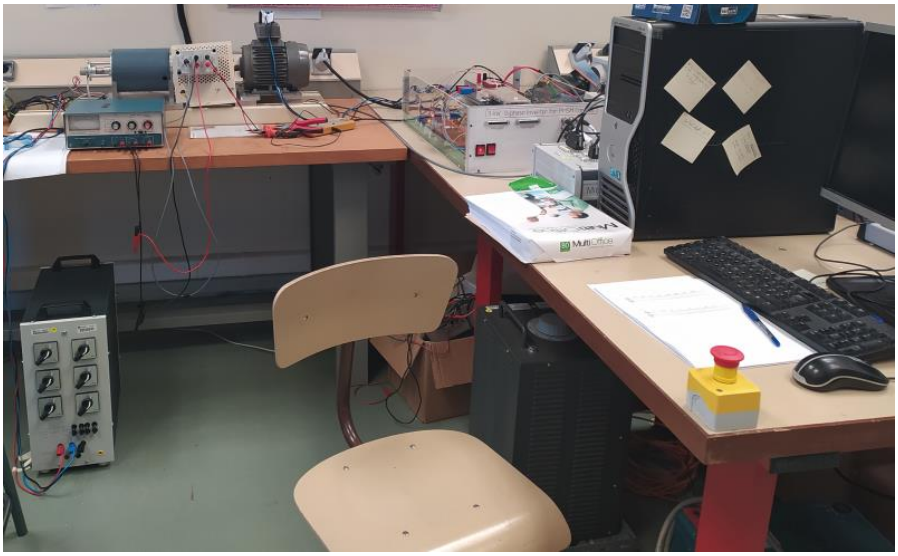

Fig. 7. Experimental hardware including power suppliers, a computer, a MicrolabBox, a three-phase inverter, and the motor

To implement the control strategy, MicrolabBox dSPACE was used. It's a compact system that offers the possibility to set up experiments quickly and easily. The MicrolabBox has more than 100 channels with different I/O types, a dual-core processor with 2 GHz, and a programmable FPGA. It is also supported by Real-Time Interface (RTI) and ControlDesk software packages to enable the linkage with Simulink.

After compiling the model on Simulink, the RTI sends the generated C code to the MicrolabBox. This code is then converted to PWM pulses in order to control the power converter. Using the analog-to-digital converter (ADC), the converter signals are supplied to the Microlabbox. It's possible to visualize online the evolution of all the obtained signals and measurements and to adjust all the parameters at run time using the Control desk monitoring software. The PMaSRM motor and the connection between the inverter and the MicrolabBox are represented in Fig. 8 and Fig. 9, respectively.

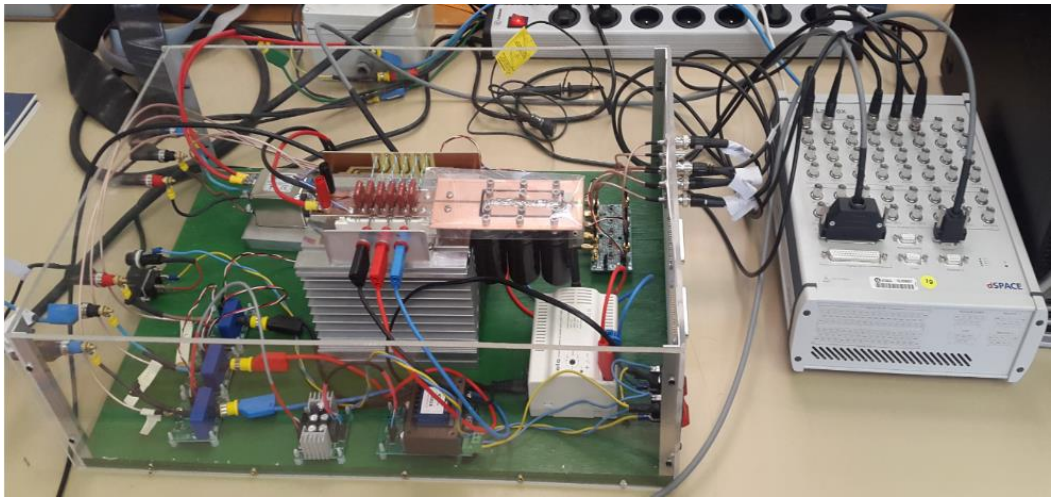

Fig. 8. The connection between the MicrolabBox dspace and the three-phase inverter

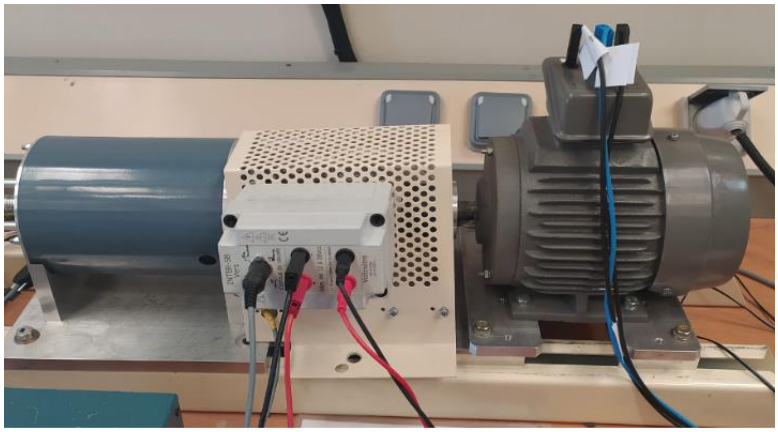

Fig. 9. The PMaSRM motor, torque sensor, IPMSM used as a load

After implementing the MTPA control strategy under a load operating mode (Tr=2.5 Nm) and applying the same speed reference as simulated, the obtained waveforms are illustrated in Fig. 10.

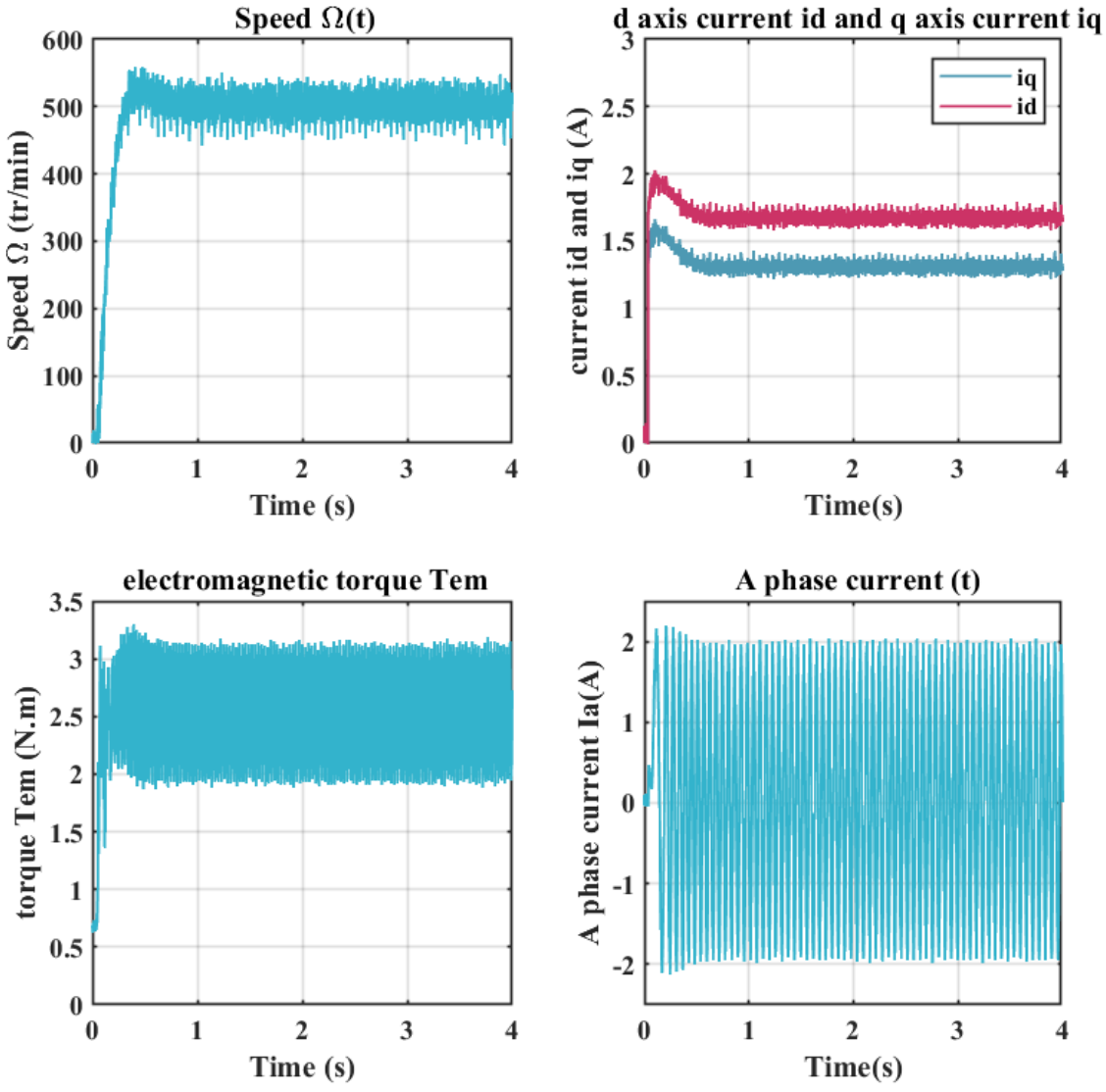

Fig. 10. Experimental Results

The actual speed reaches its reference value of 500 rpm, and the electromagnetic torque is oscillating around an average value of 2.52 Nm. The value of the measured current of the d- and q-axis in the steady-state nearly matches the results obtained in the simulation with a slight difference of 0.2 A that can be noticed. For phase stator current, it is nearly sinusoidal with an amplitude of about 2A. However, a slight deformation is witnessed. This deformation begins mainly in the interchange section between the top half of the current and the bottom half and can be caused by the dead time of MOSFETs. Compensation of this dead-time would be considered in future work.

5. Conclusion

In this study, a constant parameter MTPA control law was established to control a PMaSRM motor. After giving the mathematical model of the motor and the inverter and explaining the control strategy, the traction system model was simulated using Matlab Simulink. It has been seen from the simulation results that both current components are used with the most effective way for producing torque. To validate the proposed technique, experiments were performed on a PMaSRM previously designed and implemented for testing in a laboratory setup. PMaSRM is a motor that has the capability required for traction systems of EVs and HEVs. However, the control system needs to be improved in order to obtain a high performance under all conditions. In future work, we will improve this control strategy by applying an adaptive control in order to consider the parameter variation due to magnetic saturation and change in temperature.

References

[1] C. Cavallaro, A. O. Di Tommaso, R. Miceli, A. Raciti, G. R. Galluzzo, and M. Trapanese, "Efficiency enhancement of permanent-magnet synchronous motor drives by online loss minimization approaches," *IEEE Trans. Ind. Electron.*, vol. 52, pp. 1153–1160, 2005. https://doi.org/10.1109/TIE.2005.851595

[2] A. Consoli, G. Scarcella, G. Scelba, and A. and Testa, "Steady-state and transient operation of IPMSMs under maximum-torque-per-ampere control," *IEEE Trans. Ind. Appl.*, vol. 46, pp. 121–129, 2010. https://doi.org/10.1109/TIA.2009.2036665

[3] Y. Nakamura, T. Kudo, F. Ishibashi, and S. Hibino, "High-Efficiency Drive Due to Power Factor Control of a Permanent Magnet Synchronous Motor," *IEEE Trans. Power Electron.*, vol. 10, pp. 247–253, 1995. https://doi.org/10.1109/63.372609

[4] R. Ni, D. Xu, G. Wang, L. Ding, G. Zhang, and L. Qu, "Maximum efficiency per ampere control of permanent-magnet synchronous machines," *IEEE Trans. Ind. Electron*, vol. 62, pp. 2135–2143, 2015. https://doi.org/10.1109/TIE.2014.2354238

[5] P. Niazi, H. A. Toliyat, and A. Goodarzi, "Robust maximum torque per ampere (MTPA) control of PM-assisted SynRM for traction applications," *IEEE Transactions on Vehicular Technology*, vol. 56, no. 4 I, pp. 1538–1545, 2007. https://doi.org/10.1109/TVT.2007.896974

[6] S. Morimoto, Y. Takeda, T. Hirasa, and K. Taniguchi, "Expansion of Operating Limits for Permanent Magnet Motor by Current Vector Control Considering Inverter Capacity," *IEEE Trans. Ind. Appl.*, vol. 26, no. 5, pp. 866–871, 1990. https://doi.org/10.1109/28.60058

[7] M. Caruso, M. Lombardo, R. Miceli, C. Nevoloso, and C. Spatro, "Maximum Torque Per Ampere control algorithm for low saliency ratio interior permanent magnet synchronous motors," in *6th International Conference on Renewable Energy Research and Application,* 2017 pp. 3–8. https://doi.org/10.1109/ICRERA.2017.8191241

[8] T. Noguchi and Y. Kumakiri, "On-line parameter identification of IPM motor using instantaneous reactive power for robust maximum torque per ampere control," *Proc. IEEE Int. Conf. Ind. Technol.*, vol. 2015-June, no. June, pp. 793–799, 2015. https://doi.org/10.1109/ICIT.2015.7125195

[9] K. Li and Y. Wang, "Maximum Torque per Ampere (MTPA) Control for IPMSM Drives Using Signal Injection and an MTPA Control Law," *IEEE Transactions on Industrial Informatics*, vol. 15, no. 10, 2019. https://doi.org/10.1109/TII.2019.2905929

[10] N. Bedetti, S. Calligaro, and R. Petrella, "Self-Adaptation of MTPA tracking controller for IPMSM

and SynRM drives based on on-line estimation of loop gain," *IEEE Energy Convers. Congr. Expo. ECCE 2017*, pp. 1917–1924, 2017. https://doi.org/10.1109/ECCE.2017.8096029

[11] B. Kerdsup, N. Takorabet, and B. Nahidmobarakeh, "Design of permanent magnet-assisted synchronous reluctance motors with maximum efficiency-power factor and torque per cost," *Int. Conf. Electr. Mach. ICEM*, pp. 2465–2471, 2018. https://doi.org/10.1109/ICELMACH.2018.8506937

[12] K. Belda, "Mathematical Modelling and Predictive Control of Permanent Magnet Synchronous Motor Drives," *Trans. Electr. Eng.*, vol. 2, no. 4, pp. 114–120, 2013. http://library.utia.cas.cz/separaty/2014/AS/belda-0422285.pdf

[13] M. Tang and S. Zhuang, "On speed control of a permanent magnet synchronous motor with current predictive compensation," *MDPI energies*, vol. 12, no. 1, 2019. https://doi.org/10.3390/en12010065

[14] R. Wang, M. Huang, C. Lu, and W. Wang, "A direct three-phase AC-AC matrix converter-based wireless power transfer system for electric vehicles," *MDPI Appl. Sci.*, vol. 10, no. 7, 2020. https://doi.org/10.3390/app10072217

[15] K. Himour and K. Iffouzar, "A random PWM control strategy for a three-level inverter used in a grid connected photovoltaic system," *Int. J. Power Electron. Drive Syst.*, vol. 11, no. 3, pp. 1547–1556, 2020. https://doi.org/10.11591/ijpeds.v11.i3.pp1547-1556

[16] M. Islam, N. Raju, and A. Ahmed, "Sinusoidal PWM Signal Generation Technique for Three Phase Voltage Source Inverter with Analog Circuit & Simulation of PWM Inverter for Standalone Load & Micro," *Int. J. Renew. Energy Res.*, vol. 3, no. 3, pp. 647–658, 2013. https://www.ijrer.com/index.php/ijrer/article/view/771

[17] Y. Wang, N. Bianchi, S. Bolognani, and L. Alberti, "Synchronous motors for traction applications," in *International conference of electrical and electronic technologies for automotive*, 2017. https://doi.org/10.23919/EETA.2017.7993210

[18] V. Erginer and M. H. Sarul, "High performance and reliable torque control of permanent magnet synchronous motors in electric vehicle applications," *Elektronika ir Elektrotechnika*, vol. 19, no. 7, pp. 41–46, 2013. https://doi.org/10.5755/j01.eee.19.7.2159

[19] X. Y. Huang, J. C. Zhang, and C. M. Sun, Z. W. Huang, Q. F. Lu, Y. T. Fan, and L. Yao "A combined simulation of high speed train permanent magnet traction system using dynamic reluctance mesh model and Simulink," *Journal of Zhejiang University: Science A (Applied Physics & Engineering)*, vol. 16, no. 8, pp. 607–615, 2015. https://doi.org/10.1631/jzus.A1400284

[20] S. Huang, Z. Chen, K. Huang, and J. Gao, "Maximum Torque Per Ampere and Flux-weakening Control for PMSM Based on Curve Fitting," *IEEE Veh. Power Propuls. Conf.*, vol. 4, no. 3, pp. 3–7, 2010. https://doi.org/10.1109/VPPC.2010.5729024

[21] B. Wu and M. Narimani, "Control of Synchronous Motor Drives," in *High-power converters and AC drives*, ohn Wiley & Sons, Ltd, 2016, pp. 353–391. https://doi.org/10.1002/9781119156079.ch15

[22] J. P. Louis, *Control of Non-conventional Synchronous Motors*. John Wiley and Sons, 2013. https://doi.org/10.1002/9781118603208

[23] K. C. Odo, S. V Egoigwe, and C. U. Ogbuka, "A Model-based PI Controller Tuning and Design for Field Oriented Current Control of Permanent Magnet Synchronous Motor," *IOSR Journal of Electrical and Electronics Engineering*, vol. 14, no. August, pp. 35–41, 2019. https://www.iosrjournals.org/iosr-jeee/Papers/Vol14%20Issue%204/Series-2/E1404023541.pdf